Journal of Quantitative Spectroscopy and Radiative Transfer E-8760

A TOMOGRAPHIC METHOD FOR THE RECONSTRUCTION OF LOCAL PROBABILITY DENSITY FUNCTIONS

Y. R. Sivathanu+ and J. P. Gore
School of Mechanical Engineering
Purdue University
W. Lafayette, IN 47907-1003

(Received February 22, 1993)

Abstract-A method of obtaining the probability density function (PDF) of local properties from path integrated measurements is described. The approach uses the discrete probability function (DPF) method to infer the PDF of the local extinction coefficient from measurements of the PDFs of the path integrated transmittance. The local PDFs obtained using the method are compared with those obtained from direct intrusive measurements in propylene/air and ethylene/air diffusion flames. The results of this comparison are good.

INTRODUCTION

Deconvolution of local properties from line of sight measurements is important in a wide variety of applications such as x-ray tomography, nuclear magnetic resonance imaging, atmospheric sciences, optical inteferometry and flow field diagnostics. The methods of obtaining local properties from path integrated measurements involve the deconvolution of Radon transforms and the inversion techniques of Abel integrals. The Radon transform and its analytical solution provide the fundamental framework for a large class of deconvolution problems and their applications as reviewed by Deans.[1] Deconvolution of path integrated

+ Corresponding author

measurements requires the inverse Radon transforms. These are usually obtained by fast Fourier transform,[2] convolution back projection,[3] or series expansion methods.[4]

For axisymmetric data, the inversion methods of the Abel integral[5-7] or "onion-peeling method" have been used in conjunction with both absorption and emission measurements. The onion peeling technique was later extended to asymmetrical fields by Chen and Goulard.[8] Reconstruction tomography for the retrieval of local properties from path integrated data has been applied to problems in combustion,[9-11] inteferometry,[12,13] and plasma diagnostics.[14]

Tomography has been used for the reconstruction of mean local properties in laminar as well as turbulent flows. Chen and Goulard[8] demonstrated the feasibility of using multiray scanning to retrieve local average species concentrations and temperatures in asymmetrical fields. Santaro et al[10] applied absorption tomography to obtain mean concentrations of methane in a turbulent methane/air non reacting jet. Tomographic inversion of line of sight infrared emission measurements from flames were used by Tourin[15] and Uchimaya et al[11] to retrieve mean temperatures. Emission and absorption measurements along a path in a laminar diffusion flame have been used by Best et al[16] to retrieve the mean temperatures and concentrations.

All of the above deconvolution studies have been restricted to obtaining average local properties. Understanding of non-linear processes such as radiative transfer and finite rate chemical kinetics in turbulent

flows requires the knowledge of the probability density function (PDF) for the local properties.[17-20] There have been attempts to use fast multiangular and multiray scanning techniques to obtain single snapshots of the turbulent flow field over a small time interval. Snyder and Hesselink[21] used multiple holographic views of a transient helium jet obtained over a time period of 0.3 ms and these were subsequently inverted to obtain the helium concentration profile. Beiting[22] utilized fan beam tomography to obtain the local concentrations in a diacetyl plume. However, both these studies were attempts to show the principle of operation of fast tomography. Considerably faster scanning and data acquisition rates are needed to achieve reasonably noise-free single shot concentration profiles, even for low Reynolds number flows. To obtain converged PDFs of concentrations and temperatures in moderate Reynolds number flows, the resources needed by the above methods are beyond current hardware and software capabilities.

Based on the above observations, the objectives of the present investigation were: (1) to develop an inverse solution method based on the discrete probability function (DPF) procedure developed by us,[23] (2) to apply the inverse method to the reconstruction of the PDF of local absorption properties using path integrated measurements, and (3) to evaluate the method by comparing the deconvolution results with measurements of local PDFs in turbulent propylene/air and ethylene/air flames. Based on the encouraging results obtained in the present study, the method has the potential to be utilized in a wide variety of turbulent flow diagnostic problems.

THEORETICAL METHODS

Following our earlier work[23] the process associated with the construction of a discrete probability function (DPF) is shown in Fig. 1. The discrete probability function $P(\tau)$ of the transmittance τ consists of a finite number N of individual values τ_i, and the probability P_i of occurrence of τ in a small interval around τ_i:

$$P(\tau) = (\tau_i ; P_i),\ i=1,N; \tag{1}$$

where

$$P_i = \int_{\tau_i-\Delta\tau_i/2}^{\tau_i+\Delta\tau_i/2} PDF(\tau)\, d\tau, \tag{2}$$

and $PDF(\tau)$ is the probability density function of the transmittance. The values τ_i and $\Delta\tau_i$ are chosen such that all possible values lie within one of the N bins. Although, Fig. 1 shows uniform $\Delta\tau_i$, unevenly spaced bins may be used as well. The choice of N depends on the required resolution. $P(\tau)$ can be designed to contain the same information as the PDF to a specified accuracy by increasing the number of bins N.

The above definition of the DPF has been formalized and used in conjunction with the equation of radiative transfer to obtain the PDFs of radiation intensity leaving a path given the PDFs of local temperatures and transmittances along the path.[23] For increasing the utility of non-intrusive transmittance and emission measurements in turbulent media in conjunction with tomographic techniques, an inverse procedure of the method described by us previously[23] is needed.

Many of the popular tomographic reconstruction methods divide the axisymmetric participating medium into approximately constant property rings. The transmittance of the path crossing the outermost ring can be used to calculate the absorption coefficient directly. The transmittance of the second path consists of contribution due to the material in the two outermost rings. In order to proceed with the tomographic reconstruction process for PDFs, it is necessary to find the PDF of the absorption coefficient for the material in the second ring, given that of the material in the first ring and the PDF of transmittance for the second path. This leads to a two segment problem demonstrated in the following before its application to the overall deconvolution problem.

Deconvolution of the Transmittance PDFs for Two Segments.

The top panel of Fig. 2 shows the DPF of the transmittance $P^T(\tau)$ for a path T. This DPF is obtained from measurements of the instantaneous transmittance for the path T averaged over a sufficiently long time to reach convergence. The path T consists of two segments ΔS_1 and ΔS_2 with individual transmittances τ^1 and τ^2 such that:

$$\tau^T = \tau^1 \tau^2 \tag{3}$$

For the present problem, the DPF of the transmittance for segment 1, $P^1(\tau)$ is also known aproiri. This DPF is shown in the bottom panel of Fig. 2. In the deconvolution of axisymmetric flows, this information will be available from a measurement for the outermost ring or from the previous step in the procedure. The two DPFs in Fig. 2 contain information regarding the DPF of the transmittance of segment 2, $P^2(\tau)$ in

a convoluted form. The objective of the following steps is to extract this information. The problem can be stated as:

given

$$P^1(\tau) = (\tau^1_i ; P^1_i),\ i=1,N; \tag{4}$$

and

$$P^T(\tau) = (\tau^T_i ; P^T_i),\ i=1,N; \tag{5}$$

find

$$P^2(\tau) = (\tau^2_i ; P^2_i),\ i=1,N. \tag{6}$$

The superscripts 1, 2, and T indicate that the variables are for segments 1, 2, and the path T respectively.

The present deconvolution procedure starts with a consideration of the bins with the highest transmittance (designated i=1) in the DPFs of both segment 1 and the path T. As seen in Fig. 2, the highest transmittance for both T and 1 is unity (i.e. $\tau^1_1=1$, $\tau^T_1=1$). Clearly all possible events involving unity transmittance for the path T must originate from unity transmittance for both segment 1 and segment 2. Hence $\tau^2_1=1$ and $P^2_1 = P^T_1/P^1_1$. Naturally, the probability that the path T has a transmittance of unity is always less than or equal to the probability that path 1 has a transmittance equal to unity. The first bin in the DPF of segment 2 is thus constructed.

Simultaneous occurrences of $\tau^1_1=1$ and $\tau^2_1=1$ are convolved together to form the first bin of the DPF of the transmittance for the path T. Remaining occurrences of $\tau^2_1=1$ are convolved with other bins of $P^1(\tau)$ contribute to the probability of the appropriate bins in $P^T(\tau)$. In order to proceed with the evaluation of the probability of the second bin in

$P^2(\tau)$, it is necessary to remove the convolved occurrences of bin 1 of segment 2 with all the bins of segment 1 from $P^T(\tau)$. The resulting function is the conditional DPF (CDPF) of τ for the path T with the condition that the transmittance of segment 2 is not within bin 1 of its DPF. The CDPF is denoted by $C_{2,1}P^T(\tau)$, where the prefix $C_{2,1}$ indicates that the DPF is conditional on the exclusion of occurrences of $\tau^2{}_1$. To obtain this CDPF, the convolution of the first bin of segment 2 with all the bins of segment 1 is found out as $C^*{}_{2,1}P^T(\tau)$. The asterisk means that this function is the complement of $C_{2,1}P^T(\tau)$ in the sense that the sum of probabilities in $C^*{}_{2,1}P^T(\tau)$ and $C_{2,1}P^T(\tau)$ is 1. Using the method outlined by us in Ref. 23, this complimentary CDPF is found as:

$$C^*{}_{2,1}P^T(\tau) = (\tau^T{}_i\ ;\ C^*{}_{2,1}P^T{}_i),\ i=1,N; \tag{7}$$

where:

$$C^*{}_{2,1}P^T{}_i = \delta_i(\tau^*) \sum_{j=1}^{N} P^2{}_1\ P^1{}_j; \tag{8}$$

$$\tau^* = \tau^2{}_1\tau^1{}_j\ ,\ j=1,N; \tag{9}$$

where $\delta_i(\tau^*)$ is a statistical weight defined in the following.

If $\tau_k < \tau^* < \tau_{k+\Delta\tau/2}$; then $\delta_i(\tau^*)= 0$ for $i < k-1$ and $i > k+2$;
$\delta_i(\tau^*) = (\tau_{k+1}-\tau^*)/\Delta\tau$, for $i = k$ and $\delta_i(\tau^*) = (\tau^*-\tau_k)/\Delta\tau$ for $i=k+1$. (10)

If $\tau_{k-\Delta\tau/2} < \tau^* < \tau_k$; then $\delta_i(\tau^*)= 0$ for $i < k-2$ or $i > k+1$;
$\delta_i(\tau^*) = (\tau^*-\tau_{k-1})/\Delta\tau$, for $i=k$ and $\delta_i(\tau^*) = (\tau_k-\tau^*)/\Delta\tau$ for $i=k-1$. (11)

These statistical weights $\delta_i(\tau^*)$ distribute the probability of occurrence of τ^* within neighboring bins when the individual realizations

do not match the bin central value. The weights conserve the first moment of the distribution function. For the first bin of the complimentary CDPF, the conditional probability $C^*_{2,1}P^T_1$ is naturally P^T_1. The probabilities in the complimentary CDPF, $C^*_{2,1}P^T(\tau)$ represent the convolution of occurrences of $\tau^2_1=1$ and τ^1_j; j=1,N. These probabilities, denoted by $C^*_{2,1}P^T_i$, are to be subtracted from P^T_i to yield $C_{2,1}P^T_i$ for i=1,N. Note that the value $C_{2,1}P^T_1$ is identically zero.

The CDPF $C_{2,1}P^T(\tau)$ is shown in panel 1 of Fig. 3. Compared to the probabilities shown in Fig. 2, there is a large diminution in Fig. 3 because the probabilities associated with all occurrences of bin 1 of segment 2 have been removed from $P^T(\tau)$. This CDPF and the DPF of τ for segment 1 are used to construct the second bin in the DPF of segment 2. The transmittance value for the bin is selected as:

$$\tau^2_2 = \tau^T_2 / \tau^1_1 \tag{12}$$

Based on the rules of multiplication of DPFs in Ref. 23 the probability of occurrence of τ^2_2 is given by:

$$P^2_2 = C_{2,1}P^T_2 / P^1_1 \tag{13}$$

Thus the probability associated with the second bin in the DPF of τ for segment 2 is obtained. The CDPF shown in panel 1 of Fig. 3 involves contributions from the second and subsequent bins of the DPF of segment 2 in conjunction with all of the bins of segment 1. In order to proceed, the occurrence of transmittance τ^2_2, corresponding to the second bin of segment 2 convolved with all the bins in segment 1 should be removed from the CDPF $C_{2,1}P^T(\tau)$. This operation is achieved by first finding the

complimentary CDPF $C^*_{2,2}P^T(\tau)$ using Eqs. (7-11) with τ^2_1 and P^2_1 replaced by τ^2_2 and P^2_2. The CDPF $C_{2,2}P^T(\tau)$ is the conditional DPF for the total path with the probabilities associated with the occurrences of the first two bins of segment 2 removed. The probabilities associated with this CDPF, $C^*_{2,2}P^T_i$ are subtracted from $C_{2,1}P^T_i$ to obtain $C_{2,2}P^T_i$ for i=1,N. The CDPF $C_{2,2}P^T(\tau)$ is shown in panel 2 of Fig. 3. Naturally, the first two bins have a zero probability because of the exclusion by the conditioning discussed above.

The CDPF $C_{2,2}P^T(\tau)$ is utilized in conjunction with the DPF of segment 1 to construct the third bin of the DPF of segment 2. The conditional DPF $C_{2,3}P^T(\tau)$ is calculated using Eqs. (7-11) and the procedure is continued. The CDPF $C_{2,3}P^T(\tau)$ is shown in the bottom panel of Fig. 3.

The above procedure is continued until all the bins in the DPF of τ for segment 2 are obtained. The resulting $P^2(\tau)$ is shown in Fig. 4. With each step of conditioning, the probability in one bin of the CDPF of τ for T reaches zero and the probability of the remaining bins undergoes progressive diminution. The conditional DPF $C_{2,N}P^T(\tau)$, has the trivial value of 0 for all bins since occurrences of all possible values of τ^2 are eliminated by each successive step. During this process, the goal of reconstructing the DPF of segment 2 is accomplished as shown in Fig. 4. The same procedure can be used to find any two properties of a single segment convolved together. For instance, if the PDF of transmission and the PDF of intensity of any segment is known, then the above procedure

can be used to find the PDF of temperatures for that segment provided that the temperature and the transmission are uncorrelated.

DPF Deconvolution for the Turbulent Flame

Figure 5 shows an axisymmetric turbulent flame divided into N-1 rings and a central core. It is noted that with sufficient sampling time, the measurements of PDFs of the transmittance over a fixed distance for the individual rings are axisymmetric. The measurements can be collected at frequencies satisfying the Nyquist criterion making it suitable even for very high Reynolds number flows since only one channel of information is required at any one time. The number of rings can be increased to obtain a required spatial resolution within the constraints of the measuring instrument. Transmittance measurements are conducted for paths crossing the one or more rings to obtain DPFs of the transmittance $P1$, $PT2$, $PT3$,..., PTN. In general the extinction coefficient of the material within each of the rings fluctuates with time and space leading to the PDFs of transmittances for the paths 1 to TN. However, the number of rings and the width of each ring are chosen to satisfy the condition that within each ring, the extinction coefficient is a function of time only to a desired accuracy. The turbulent mixing and combustion processes result in the formation of species that absorb and scatter light. In the axisymmetric geometry of a turbulent jet flame, these processes can be made ergodic to any desired order of moment of the PDF. Thus, in the limit of the desired accuracy, PDFs of extinction coefficient for all individual rings are independent of sampling time and the azimuthal angle.

In order to utilize the measurements of DPFs of transmittance for the N paths shown in Fig. 5 to find the DPFs of local extinction coefficient (for a specified local segment length over which the extinction coefficient is constant), the two segment deconvolution procedure described in the previous section is to be successively applied. Based on the measurements of transmittance for the outermost ring $P^1(\tau)$, the DPF of the local extinction coefficient of the ring is constructed using our earlier approach[23] for obtaining the DPF of a function F(X,Y) from those of X and Y. In the present problem, the function F is defined as the local extinction coefficient a^1 which depends on the transmittance τ^1 over the distance ΔS_1:

$$F(\tau^1{}_i) = -\ln(\tau^1{}_i) / \Delta S_1 = a^1{}_i \qquad (14)$$

Using the measured DPF $P^1(\tau)$, the DPF of local extinction coefficient $P^1(a)$ is obtained. The path T2 over which the next set of transmittance measurements are obtained consists of three segments. Two of these segments are formed by material from the outermost ring and are of identical length $\Delta S^1{}_2/2$. The DPF of the combined transmittance of these segments is constructed using the DPF of extinction coefficient for ring 1 $P^1(a)$ using the procedure outlined in Ref. 23.

$$F(a^1{}_i) = \exp(-a^1{}_i \Delta S^1{}_2) = \tau^1{}_{2i} \qquad (15)$$

Hence the DPF of $\tau^1{}_{2i}$ is found from that of $a^1{}_i$. The path T2 effectively consists of two segments, one with a known DPF of transmittance and a second with a DPF of transmittance yet to be determined. The two segment approach described in the previous section is readily applicable to yield the DPF of the transmittance for the segment ΔS_2. The DPF of

extinction coefficient a^2 for the material in ring 2 is calculated from that of transmittance over ΔS_2.

The path T3 over which the next transmittance measurements are obtained consists of 5 segments. Two out of these have lengths $\Delta S^1{}_3/2$ and extinction coefficients a^1, the DPF of which was found earlier. Two of the remaining segments have lengths $\Delta S^2{}_3/2$ and extinction coefficient a^2, the DPF of which was found as described in the preceding paragraph. The fifth segment has the properties of ring 3 which are yet to be found. The problem is reduced to a two-segment problem by combining the four segments with known DPFs of absorption coefficients into a combined segment SC. The DPF of transmittance for the combined segments is found using the procedure described by us in Ref. 23 as follows:

$$P^{SC}(\tau) = (\tau^{SC}_i ; P^{SC}_i); \; i=1,N; \tag{16}$$

where

$$\tau^{SC} = \tau^2{}_k \tau^1{}_j; \; j=1,N; \; k=1,M; \text{ and} \tag{17}$$

$$\tau^2{}_k = \exp(-a^2{}_k \, \Delta S^3{}_2); \; k=1,M; \text{ and} \tag{18}$$

$$\tau^1{}_j = \exp(-a^1{}_j \, \Delta S^3{}_1); \; j=1,N; \text{ and} \tag{19}$$

$$P^{SC}_i = \delta_i(\tau^{SC}) \sum_{k=1}^{M} \sum_{j=1}^{N} P_j^{\,1} \, P_k^{\,2}; \tag{20}$$

where $\delta_i(\tau^{SC})$ is the statistical weights described by Eqs. (10-11). N and M are the number of bins in the DPF of extinction coefficients for ring 1 and ring 2.

The problem is now reduced to a two-segment problem involving the segment SC with a DPF of transmittance known from the above procedure

and the combined path T3 whose DPF of transmittance is measured. Hence the DPF of transmittance for the portion of ring 3, ΔS_3 included in the path T3 can be calculated. This DPF of transmittance is converted to that of the extinction coefficient for material in ring 3, a^3, using the procedure described above.

Similarly for any path M, the information concerning the DPFs of extinction coefficients for the outer M-1 rings are used to compute the DPF of transmittance for the part of the path consisting of portions of these rings. This DPF combined with the measurements for the path M yield the DPF of the local transmittance and the extinction coefficient for ring M. This procedure is repeated until the transmittance measurement for the path TN, which passes through the axis of the flame, is utilized to find the DPF of extinction coefficient for the central core.

RESULTS AND DISCUSSION

The method described above was validated by comparing the deconvoluted DPFs of local extinction coefficient with measurements obtained using a purged optical probe.[19] A highly buoyant flame burning propylene in air on a 50 mm diameter burner with an exit Reynolds number of 670 studied by us[24] as well as a jet flame with a 6 mm diameter, 9200 exit Reynolds number and ethylene burning in air were used.

For the propylene/air flame, PDFs of local extinction coefficient obtained with 6 mm diameter purged light guides at x/d=6.7 for a

wavelength of 632.8 nm are available from Ref. 24. However, transmittance measurements for paths 1-TN are not available. In order to proceed, the path integrated data were generated synthetically from the local data using the DPF method for the equation of transfer described by us.[23] Local measurements were available for 12 positions spaced 7 mm apart from the center-line to the edge of the flame.

The advantage of synthesizing the path integrated data is that the PDF deconvolution procedure can be evaluated independent of the errors caused by the underlying difficulties of: (1) spatial correlation between adjoining rings, (2) electronic noise in the detectors, and (3) ambiguity concerning centerline and true axisymmetry. The synthetically generated DPFs are free of these difficulties allowing a clear evaluation of the deconvolution procedure. It is important to demonstrate the procedure for the noise-free data since this is the first time that the DPF method[23] has been applied to an inverse problem.

Figure 6 shows the PDFs of the local extinction coefficient for the propylene/air flames at three radial positions at x/d=6.7. The histogram represents the local measurements and the solid line represents the deconvoluted results from the synthetic path integrated data. As can be seen from the excellent agreement, the present method is successful in reproducing the PDFs of local extinction coefficient by deconvolution of synthetic path integrated data. With this success, the method is tested by using actual transmittance measurements.

Transmittance measurements for chord like paths separated by 5 mm were completed at x/d = 30 for the ethylene/air diffusion flame. The PDFs of these data for four representative paths are shown in Fig. 7. The flame half-width at this axial location was 50 mm providing a total of 11 path integrated measurements. The shape of the PDF changes from nearly Gaussian at the center to highly intermittent near and beyond r=30 mm. For evaluating the results of the deconvolution procedure, measurements of local extinction coefficient at several positions using the optical probe were also completed. These measurements were conducted with a spatial resolution of 10 mm to provide sufficient absorption along the path to improve the accuracy of the measurements. The experimental uncertainties in the first two moments of the PDF are less than 10% for positions close to the center, while at the edge of the flame (r = 50mm), these uncertainties increase to about 40%.

Figure 8 shows the PDFs of the extinction coefficient at four different radial positions obtained from the deconvolution procedure (Decon.) and from the local measurements (Probe). The resolution of the DPF procedure is set at 10 mm to match that of the probe measurements allowing this comparison. The effects of noise introduced by the experiment and by the deconvolution procedure are observed particularly at the r=20 mm position. However, the overall agreement between the two is reasonably good. These results provide confidence in the new procedure for obtaining PDFs of local absorption properties based on those of path integrated measurements.

In the present paper, the deconvolution procedure for PDFs is developed and evaluated for spatially uncorrelated discretization. The spatial resolution of the procedure can be improved significantly by conducting closely spaced transmittance measurements and using the spatially correlated DPF method described in an Appendix in our previous work.[23]

CONCLUSIONS

A deconvolution procedure for obtaining the local PDFs of extinction coefficients from path integrated measurements is described. The new method allows local extinction measurements of PDFs for optically thin (relatively) and thick media in turbulent flows. The method has been validated using experimental data. Further work is necessary to utilize the full potential of the method by conducting spatially correlated measurements and deconvolutions.

REFERENCES

1. S. R. Deans, The Radon Transform and Some of its Applications, Wiley, New York (1983).
2. L. A. Shepp and B. F. Logan, IEEE Trans. Nucl. Sci. **NS-21**, 21 (1974).
3. G. N. Ramachandran and A. V. Lakshminarayanan, Proc. Nat. Acad. Sci. **68**, 2236, U.S. A. (1970).
4. M. Ravichandran and F. C. Gouldin, Appl. Opt. **27**, 4084 (1988).
5. H. R. Griem, Plasma Spectroscopy, McGraw-Hill, New York (1964).
6. W. C. Barr, J. Opt. Soc. Am. **52**, 885 (1962).

7. J. Glasser, J. Chapelle, and J. C. Boetlner, Appl. Opt. **17**, 3750 (1960).

8. F. P. Chen and R. Goulard, JQSRT **16**, 819 (1976).

9. P. J. Emmerman, R. Goulard, R. J. Santaro, and H. G. Semerjian, J. Energy **4**, 70 (1980).

10. R. J. Santaro, H. G. Semerjian, P. J. Emmerman, and R. Goulard, Int. J. Heat and Mass Trans. **24**, 1139 (1981).

11. H. Uchimaya, M. Nakajima, and S. Yuta., Appl. Opt. **24**, 4111 (1985).

12. D. W. Sweeny and C. M. Vest, Appl. Opt. **12**, 2649 (1973).

13. C. M. Vest and I. Prikryl, Appl. Opt. **23**, 2433 (1984).

14. M. Hino, T. Aono, M. Nakajima, and S. Yuta, Appl. Opt. **62**, 4742 (1987).

15. R. H. Tourin, Spectroscopic Gas Temperature Measurement, Elsevier, New York (1983).

16. P. E. Best, P. L. Chien, R. M. Carangelo, P. R. Solomon, M. Danchak, and I. Ilovici, Combust. Flame **85**, 309 (1991).

17. G. M. Faeth, J. P. Gore, S. G. Chuech, and S. M. Jeng, Ann. Rev. Num. Fluid Mech. Heat Trans., vol 2, pp. 1-38, C. L. Tien and T. C. Chawla eds., Hemisphere, New York (1986).

18. R. Viskanta and M. P. Menguc, Prog. Energy Comb. Sci. **13**, 97 (1987).

19. Y. R. Sivathanu, J. P. Gore, and J. Dolinar, Combust. Sci. Technol. **76**, 45 (1991).

20. S. B. Pope, Twenty-Third Symposium (International) on Combustion, pp. 591-612, The Combustion Institute, PA (1990).

21. R. Snyder and L. Hesselink, Optic Let. **13**, 87 (1988).

22. E. J. Beiting, 28th Aerospace Sciences Meeting, **90**-0157, AIAA, Washington, D.C. (1990).

23. Y. R. Sivathanu and J. P. Gore, JQSRT, in press (1993).

24. Y. R. Sivathanu and J. P. Gore, J. Heat Trans. **114**, 659 (1992).

List of figures:

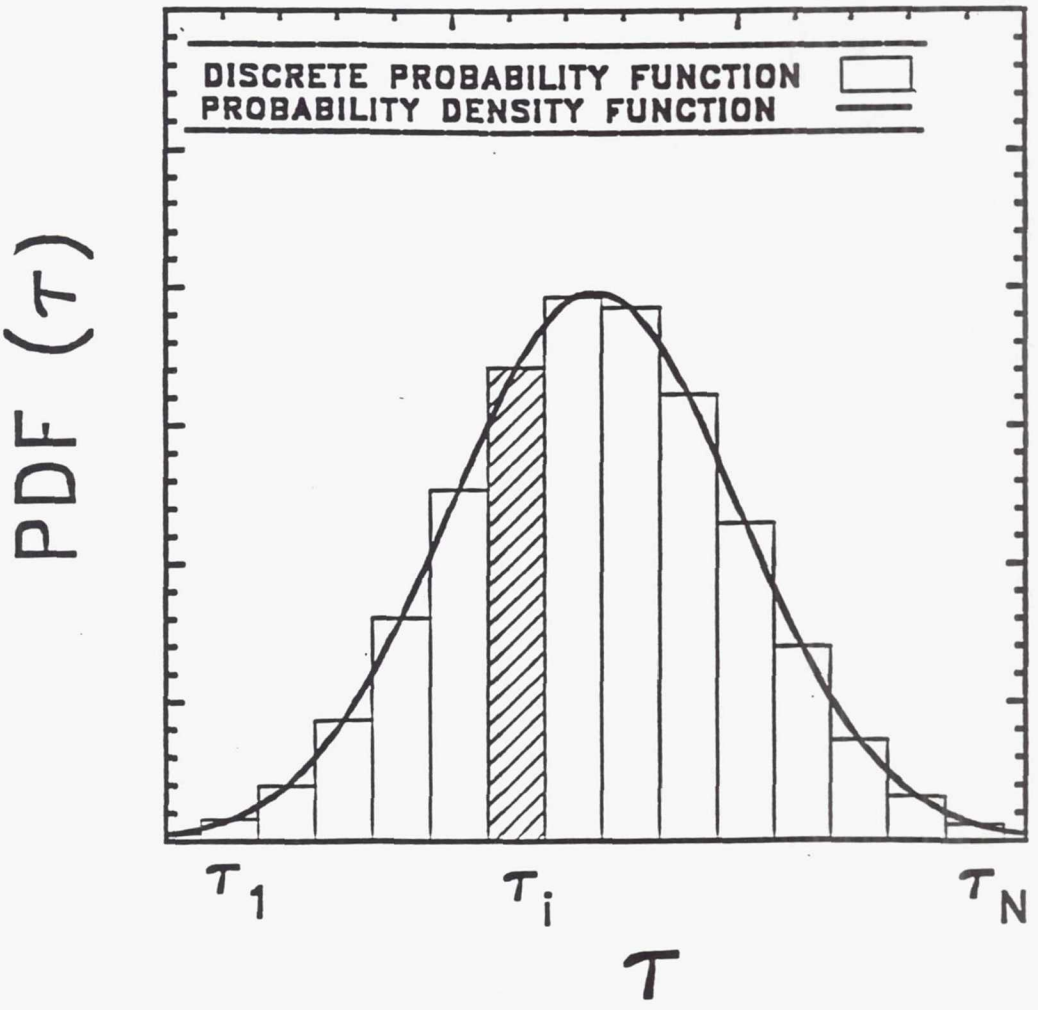

-- Figure 1: Sivathanu and Gore

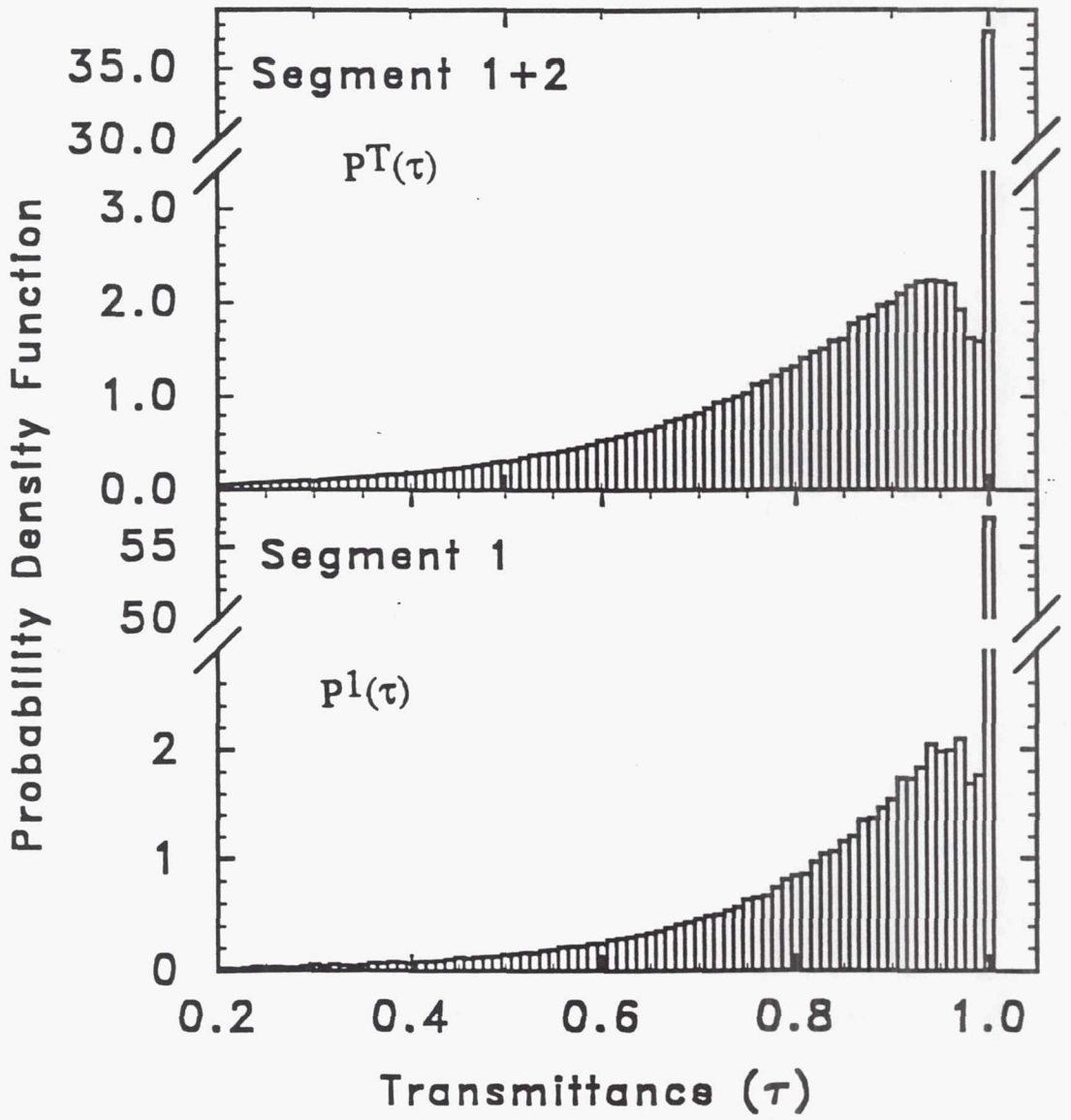

Fig. 2 Sivathanu and Gore

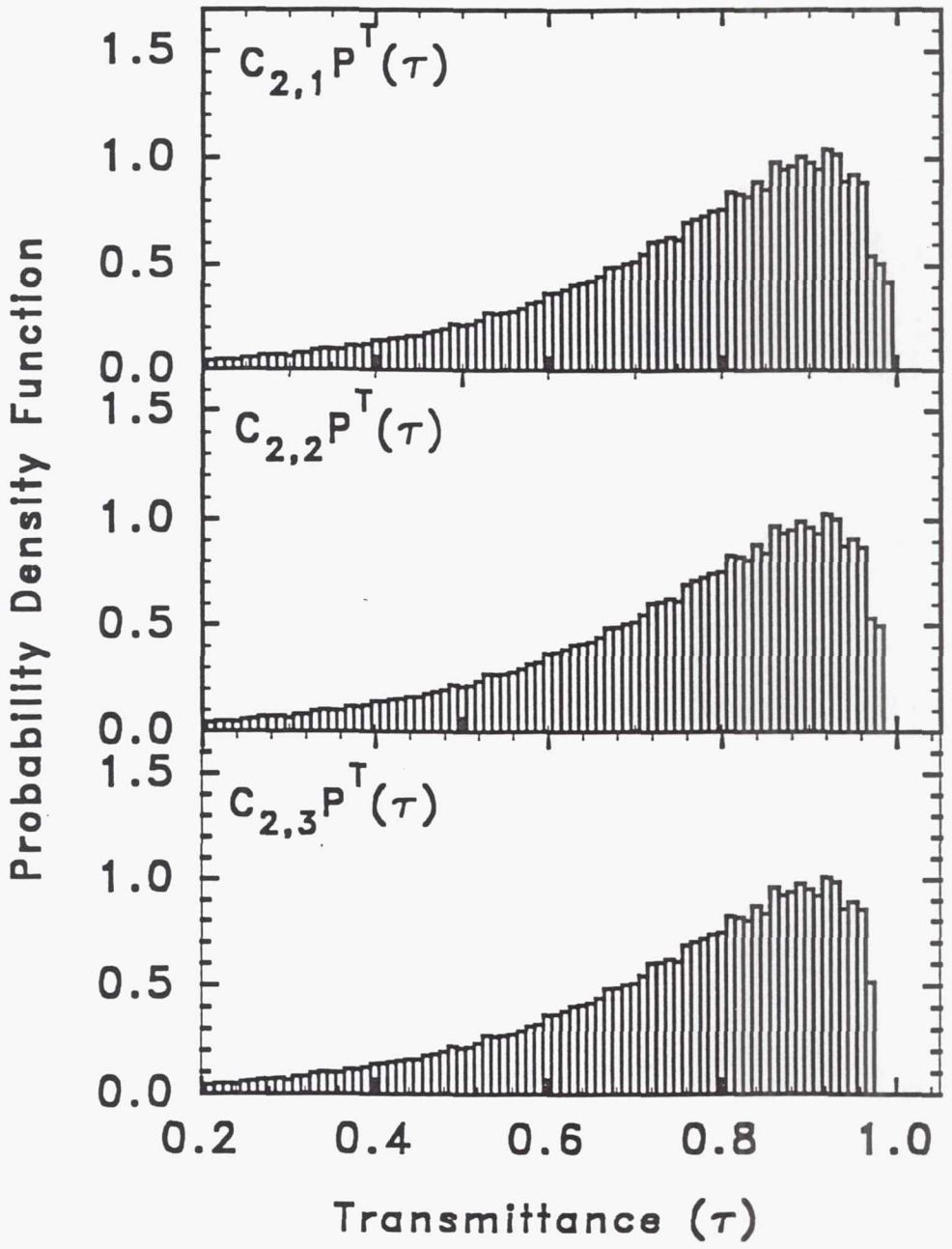

Fig. 3 Sivathanu and Gore

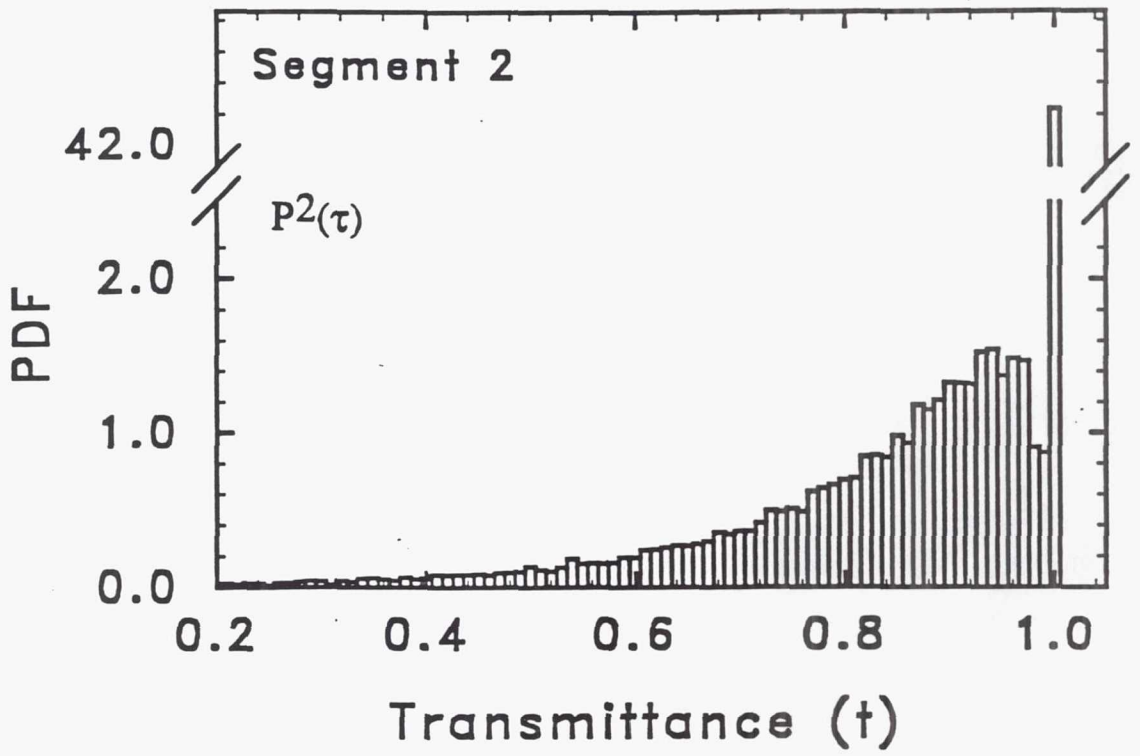

Figure 4 Sivathanu and Gore

DECONVOLUTION USING THE DPF METHOD

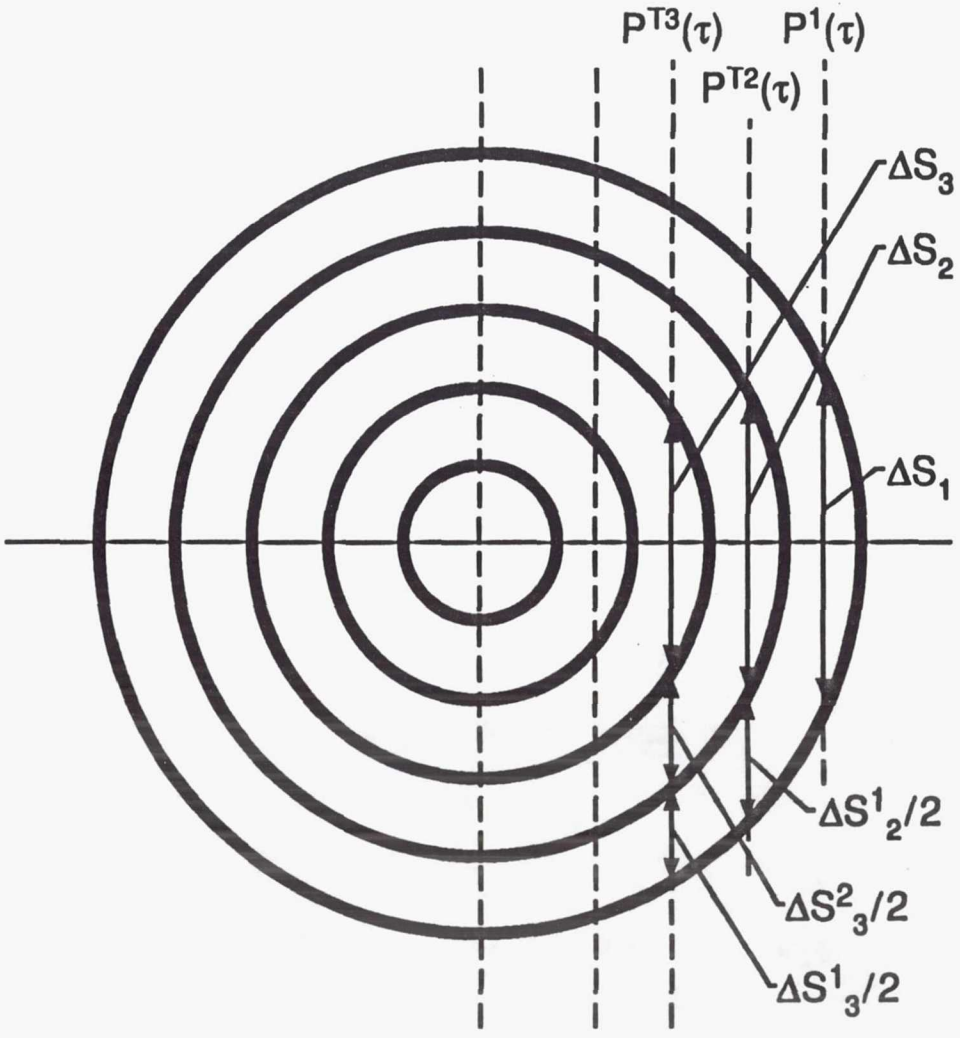

MEASUREMENTS:

$P^1(\tau) \equiv (\tau^1{}_i, P^1{}_i)$; i = 1,N

$P^{T2}(\tau)$, $P^{T3}(\tau)$, etc.

FIND

$P^2(\tau)$, $P^3(\tau)$, etc.

Figure 5 Sivathanu and Gore

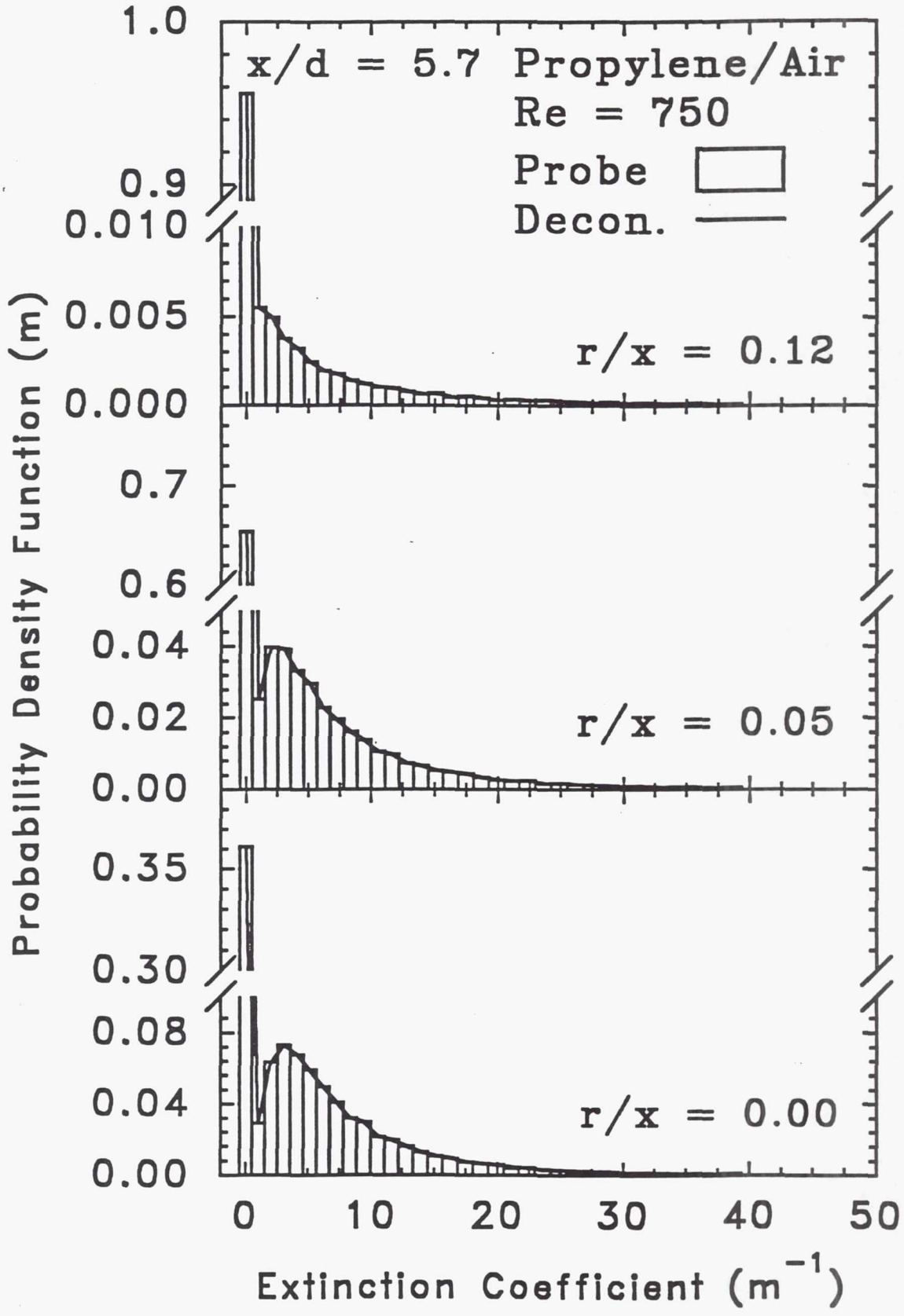

Figure 6 Sivathanu and Gore

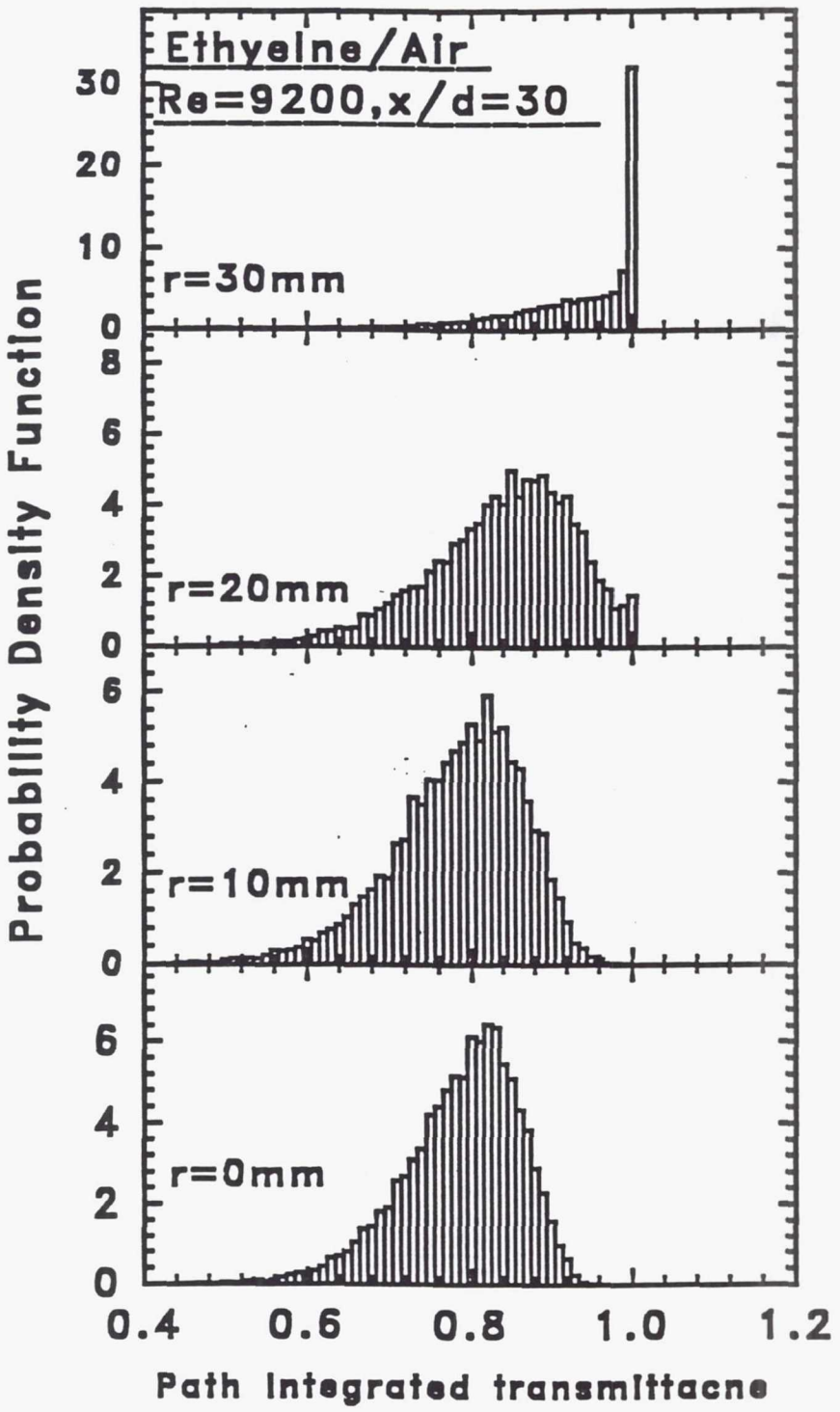

Fig. 7 Sivathanu and Gore

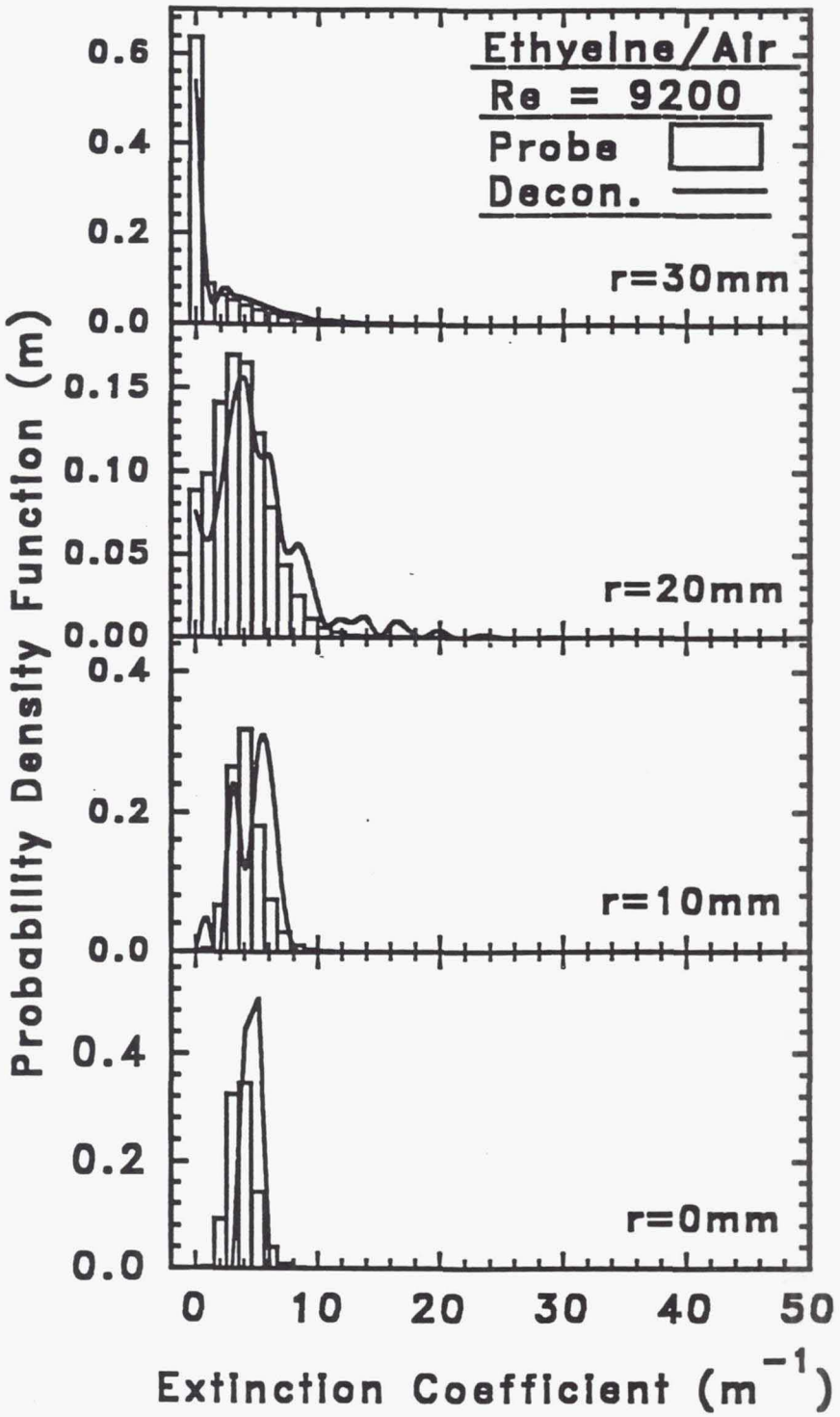

Fig. 8 Sivathanu and Gore